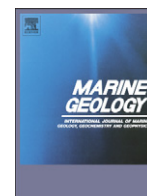


Contents lists available at ScienceDirect

Marine Geology

journal homepage: www.elsevier.com/locate/margeo

Cold seep carbonates and associated cold-water corals at the Hikurangi Margin, New Zealand: New insights into fluid pathways, growth structures and geochronology

Volker Liebetrau*, Anton Eisenhauer, Peter Linke

IFM-GEOMAR, Leibniz Institute of Marine Sciences at the University of Kiel, East Shore Campus, Wischhofstrasse 1-3, D-24148 Kiel, Germany

ARTICLE INFO

Article history:

Received 12 April 2009

Received in revised form 27 November 2009

Accepted 1 January 2010

Available online xxx

Keywords:

Hikurangi Margin
cold seeps
authigenic carbonates
U–Th geochronology
fluid pathways
cold-water corals

ABSTRACT

The aim of this study is to provide combined new insights into the geochronological framework, isotope geochemical signatures and structural observations of methane related authigenic carbonate settings and associated cold-water corals from offshore New Zealand. The analysed samples are obtained from calcified sediments of three different cold seep areas at the Hikurangi Margin: Opouawe Bank, Uruti and Omakere Ridge. We focused the sub-sampling on aragonitic precipitates in vein like structures, partly still open fluid channel systems and related chemoherm structures in order to identify the timing and signature of focused marine methane emanation. The presented initial U/Th age data set indicates different generations of intensified seep activity and related carbonate precipitation between $12,400 \pm 160$ and 2090 ± 850 years BP. The youngest stage so far, was identified as contemporaneous cold seep activity at the southernmost (North Tower, Opouawe Bank) and northernmost (Bear's Paw, Omakere Ridge) sampling sites around 2300 years BP. Sharing the same water depth (1050 to 1100 m) these sites imply regional margin-wide tectonic or hydrological changes as controlling process.

An intermediate phase of vein and channel structures within the sediment was detected for a time interval between approximately 5000 and 4000 years BP with contemporaneous settings of focused seep activity around 4300 years BP at Uruti Ridge (LM-10) and Opouawe Bank.

$\delta^{13}\text{C}_{\text{PDB}}$ data reflect site and carbonate type specific signatures, clustering around -52% (Uruti and Omakere Ridge) and -47% for the fluid pathway system and the uppermost surface at North Tower site (Opouawe Bank). Late stage precipitates in chemoherm cavities of the latter reflect significantly heavier values of about -38% . Porous precipitates within open fluid channel systems are characterized by decreased $\delta^{234}\text{U}_{(T)}$ values, exceptional high Th and U concentrations and slightly lighter $\delta^{13}\text{C}_{\text{PDB}}$ signatures when compared to adjacent rim-like and dense cements. This specific kind of precipitate is interpreted as indicator for phases of less vigorous fluid seepage.

The observed occurrence of cold-water corals seems to be mostly depending on the abundance of authigenic carbonates as a substrate exposed to erosive bottom water currents. But, seafloor observations combined with preliminary age data indicate a significant time gap between the inferred end of cold seep activity and coral colonization. U–Th analyses of recent reef-forming coral provided an initial $\delta^{234}\text{U}_{(0)}$ value of $146.3 \pm 3.9\%$ and 0.0013 ± 0.0002 as starting $^{230}\text{Th}/^{234}\text{U}$ activity ratio for coral growth in the bottom water.

© 2010 Elsevier B.V. All rights reserved.

1. Introduction

Authigenic carbonates from cold seeps are potential high-resolution recorder of changes in venting activity and fluid composition through time (e.g. Teichert et al., 2003; Campbell, 2006; Judd and Hovland, 2007); they may or may not be associated with gas hydrates (Teichert et al., 2005). Various examples from modern and ancient cold seeps have been described from continental margins

worldwide (e.g. Kulm and Suess, 1990; Campbell et al., 2002; Nymann et al., this issue). After a decade of microbiological and geochemical studies, we know that in marine cold seep environments, methane and other hydrocarbon compounds contained in the ascending fluids are oxidized to bicarbonate (HCO_3^-) by a microbial consortium of sulphate-reducing bacteria and methanotrophic archaea (Boetius et al., 2000). Anaerobic oxidation of methane is the main microbial process driving the precipitation of authigenic carbonate build-ups within subsurface anoxic sediments and the bottom water. This process explains why the seafloor is often cemented by carbonate at sites of active methane seepage, either as chemoherm structures associated to focussed fluid venting that grow into the water column,

* Corresponding author. Tel.: +49 431 6002117; fax: +49 431 6002928.

E-mail addresses: vliebetrau@ifm-geomar.de (V. Liebetrau), aeseinhauer@ifm-geomar.de (A. Eisenhauer), plinke@ifm-geomar.de (P. Linke).

or as carbonate cementations/concretions in the sediment. The lateral and vertical extents of these methane-derived authigenic carbonates are controlled by the balance between the intensity of the fluid flux and the ability of microbes to oxidize methane and reduce sulphate (Luff and Wallman, 2003). The efficiency of this process (Sommer et al., 2006) might not be sufficient enough for high methane flux (in dissolved and especially gaseous phase), so that methane can escape into the water column and may eventually reach the atmosphere (e.g. Sauter et al., 2006). Numerical modelling of carbonate crust formation has shown that bioturbation and sedimentation rates are additional important factors in controlling the flow of water and methane, and thus carbonate precipitation at cold seep sites (Luff et al., 2004).

The carbonate build-ups observed at the seafloor exhibit various morphologies: massive to porous crusts centimeter to meters thick that form large pavements or fragmented slabs, circular chimneys, and irregular concretions corresponding to cemented bioturbation traces. These hard substrates are often inhabited by an abundant motile fauna (bivalves, gastropods, crustaceans, fishes etc.) and colonized by fixed organisms such as tubeworms and cold-water corals, which may become entombed as biotic elements in the seep carbonates (e.g. Campbell et al., this issue).

Mineralogy, geochemical and isotopic signatures of authigenic carbonates depend on the composition of the ascending fluids and the environmental conditions during formation. These studies together with U–Th age constraints on paleo-seepage activity are crucial tools for the identification and understanding of the driving processes, mechanisms and sources of marine methane emanation (Teichert et al., 2003; Kutterolf et al., 2008; Watanabe et al., 2008; Bayon et al., 2009). Cold seep carbonates are in particular suitable for the reconstruction of marine methane emanation and estimates of their contribution to the marine and global carbon cycle (Aloisi et al., 2002; Judd et al., 2002; Judd, 2003).

Cold-water coral habitats occur in a wide range of geological settings and different ecosystems, a compilation is presented by Roberts et al. (2009). With respect to cold seep environments, the investigation of associated cold-water corals may provide important constraints on the impact of fluid emanation on the bottom water chemistry, supporting quantification and reconstruction attempts. Furthermore, a combination of contemporaneous cold-water coral and cold seep carbonate archives would be especially useful for the calibration of isotope proxies for carbonate precipitation conditions of cold seep environments in the past.

According to a hypothesized relationship between the occurrence of cold-water corals and hydrocarbon seepage (Hovland and Thomsen, 1997) and contradictory findings (Becker et al., 2009) our approach is focused on the geochronology of cold-water coral occurrence and cold seep activity. Additionally, the detection of age gaps between coral growth and formation of the underlying hard substrate could provide information about the time interval required for coral settlement and potentially related changes of hydrodynamic controls (Mienis et al., 2007; Roberts et al., 2006; White et al., 2005).

RV SONNE cruise SO191 to the Hikurangi Margin (Bialas et al., 2007) provided ideal samples of seafloor carbonate pavements and cold-water corals, which were recovered with a large video-guided grab (TVG). Cross-cuts through these large (up to $1.8 \times 1.2 \times 1$ m)

blocks from three different sampling areas (Fig. 1A, Table 1) provide a geochronological, geochemical, mineralogical and structural view into carbonate precipitation processes at the seafloor and the development of the fluid 'plumbing' system through time.

The detailed investigation of cold seep carbonates from the tectonically highly active Hikurangi Margin fills a gap in the over-regional view on circum-Pacific cold seep areas of different geological settings like Hydrate Ridge (mature accretionary system), offshore Costa Rica (erosive subduction) and the South China Sea (passive continental margin).

On regional scale the investigation of fluid pathway structures and the timing of intensified fluid emanation contributes to the assessment of direct fluid flux measurements at active seep sites (Linke et al., this issue), when compared to the past. Furthermore, it supports interpretation and understanding of cold seep structures recovered on land on the North Island of New Zealand (Nymann et al., this issue).

2. Regional setting and sampling sites

The Hikurangi Margin at the east coast of New Zealand's North Island is characterized by the oblique subduction of the Pacific plate beneath the Australian plate (Fig. 1). The convergence rate varies from 45 mm yr^{-1} in the North Island region to 38 mm yr^{-1} in the northern South Island region forming a large accretionary prism with a series of accretionary ridges with active cold seeps offshore and fossil ones onshore (Barnes et al., this issue; Campbell et al., 2008; Lewis and Marshall, 1996).

Fossil cold seeps are described for northern Wairarapa (Lederset et al., 2003) and large tubular carbonate concretions (50–85% carbonate) with near-central conduits are interpreted as part of a subsurface plumbing network of a paleo cold seep system in coastal cliffs north of Cape Turnagain (Nymann et al., this issue). These findings demonstrate that fluid venting at the Hikurangi Margin is a long lasting phenomenon.

In this study we focus on the analyses of carbonate samples obtained from three study areas during SONNE cruise SO191 – Opouawe Bank, Uruti and Omakere Ridge (Fig. 1) in order to cover different settings along the Hikurangi Margin. All seep sites lie on separate crests of thrust-faulted ridges at mid-slope depths (Barnes et al., this issue). They are positioned near the seaward edge of the Cretaceous and Paleogene basement rocks, which constitute a relatively impermeable backstop that focuses fluid migration offshore today along low-angle thrust faults and the décollement (c.f. Lewis and Marshall, 1996; Barnes et al., this issue). Fault fracture networks are visible in seismic images beneath the seeps, and bottom simulating reflectors (BSR) are disturbed at these locations by upward fluid and gas migration to the seafloor seep sites (Barnes et al., this issue; Netzeband et al., this issue).

2.1. Opouawe Bank

The Opouawe Bank is one of the accretionary ridges culminating in about 900 m water depth and well separated from the continental slope by erosive canyons (c.f. Klaucke et al., this issue). High-resolution side-scan sonar data collected over Opouawe Bank indicated thirteen different cold seeps (Greinert et al., this issue), which Klaucke et al. (this issue) divide into two types: high acoustic

Fig. 1. Compilation of bathymetry, site distribution and seafloor observation during the deployment of TV-guided grabs, RV SONNE cruise SO191. A: Overview map showing the bathymetry of the Hikurangi Margin at the east coast of New Zealand's North Island. The squares mark the sampling areas of this study. Lake Taupo appears in light grey in the central part of the island. B: Typical seafloor observation of cold seep faunal community and blocks of less mature calcified sediments at Bear's Paw (Omakere Ridge). C: The white square marks the recovered sample at station # 165 (each picture width: approx. 2 m). D: Sampled cold-water coral reef structures (station # 227) on top of authigenic carbonates at the Moa site of Omakere Ridge (picture width approx. 2 m). Insertion shows enlargement of a recovered fragment (white square) of a living reef-forming colony. E: Flat, fractured and mature calcified pavement-like seafloor at the top of Uruti Ridge close to the LM-10 site (station # 316). The white square marks the recovered solid block (picture width approx. 2 m). F: Characteristic high relief seafloor with large separated blocks and chemoherm structures indicating pronounced exposure due to erosional conditions at the North Tower site of Opouawe Bank. The white square marks the sampled block at station # 138 (pict. width: approx. 4 m). G: Enlarged documentation of the upright in-situ position of the largest cold seep carbonate sample recovered since (station # 138, picture width approx. 2.5 m).

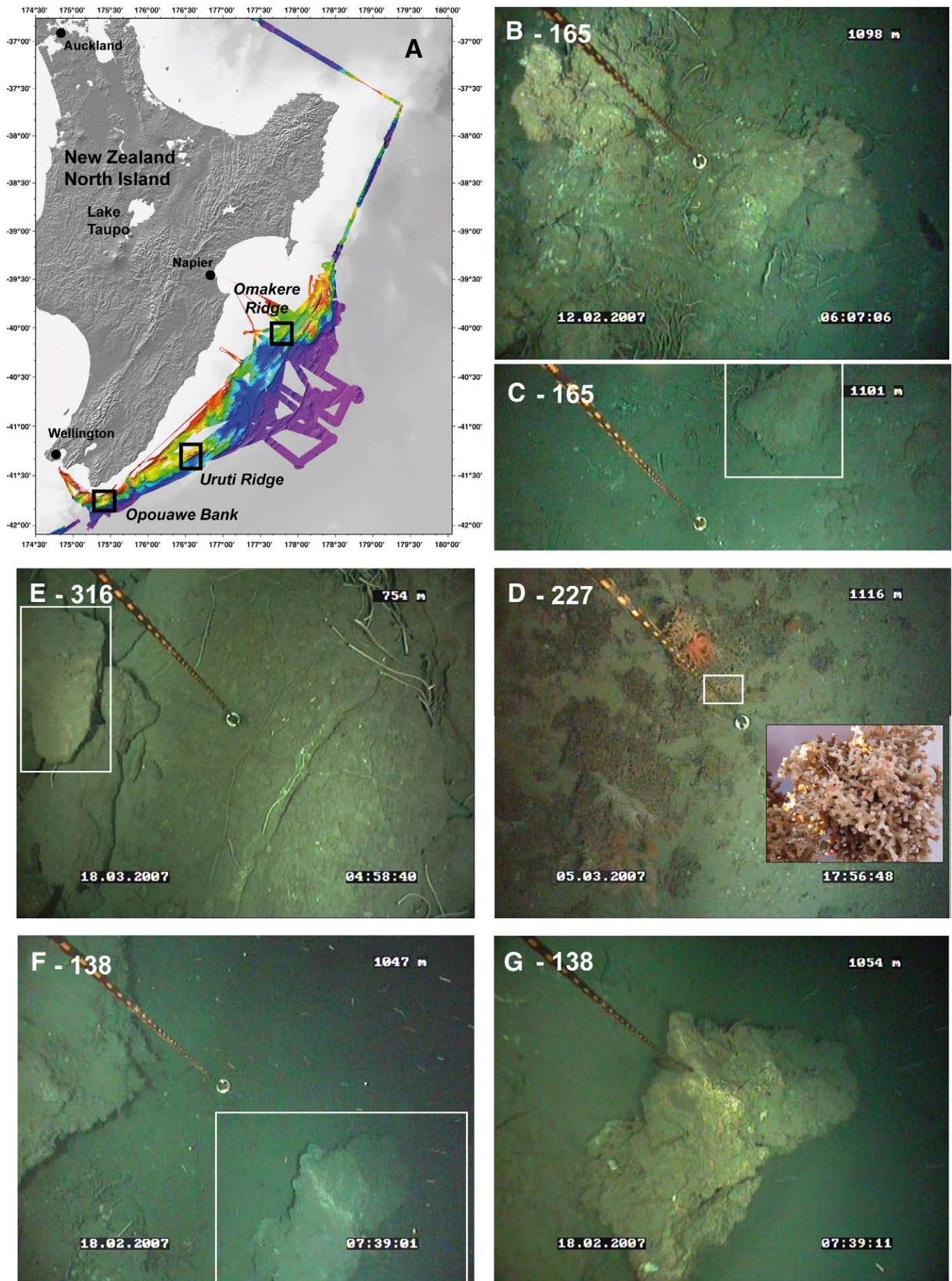


Table 1
List of stations and samples relevant for this paper.

Area site	Position	Water depth	Habitat	Number of sub-samples
<i>RV Sonne, cruise 191, station #</i>	Latitude (S), longitude (E)	(m)	Description based on TV-guided grab	
<i>Opouawe Bank North Tower</i> 138	41°46.908 175°24.092	1047	Cold seep, large carbonate blocks, chemoherm structures, cold-water corals associated	11
<i>Uruti Ridge LM-10</i> 316	41°17.530 176°32.870	756	Cold seep, flat pavement-like seafloor, dense sediment	3
<i>Omakere Ridge Bear's Paw</i> 165	40°03.185 177°49.264	1102	Cold seep, small blocks, less dense porous sediment, rich in cold seep fauna remnants	2
<i>Omakere Ridge Moa</i> 218	40°03.270 177°48.770	1107	Cold-water coral reef on inactive seep site, reef formation terminated	2
227	40°03.280 177°48.75	1120	Cold-water coral reef, reef colony alive	1

backscatter intensity patches with apparent relief, and patches with moderate backscatter and smooth to no relief. The North Tower seep site sampled in this study (1056 m water depth, Fig. 1F) belongs to the first type with a distinct clustering of individual carbonate blocks surrounded by some scattered blocks (c.f. Klaucke et al., this issue). The seep is located at the base of a 30 m-high normal fault scarp (Law et al., this issue). Visual site descriptions for the Opouawe Bank can be found in Baco et al., this issue, Law et al., this issue, and Klaucke et al., this issue. Almost vertical polygonal faults are assumed to represent the main structural control on the focused fluid flow at the Opouawe Bank.

2.2. Uruti Ridge

Uruti Ridge lies on the middle slope off the Wairarapa coast, where the offshore part of the imbricate wedge is about 90 km wide (Barnes et al., this issue). Three seep sites, including LM-10, are located at small mounds or knolls on the anticlinal crest of the thrust-faulted ridge in about 800 m water depth and in close proximity to the eastern end of a major strike slip fault. The seep sites are characterized by strong back scatter in side-scan sonar images and acoustic flares in the water column (Greinert et al., this issue). Visual site inspection revealed that the knolls are similar in form and consist of a summit with moderate-relief. The summits consist of authigenic carbonate rocks, often in the form of a relatively flat and wide pavement. The flanks show isolated carbonate blocks as talus before the background soft sediment habitat becomes dominant at the feet of the knolls (c.f. Baco et al., this issue). The TV-guided grab was successfully deployed at the fractured rim of the flat summit of the LM-10 site at Uruti Ridge (756 m water depth, Fig. 1E).

2.3. Omakere Ridge

Multibeam bathymetry offshore Napier at the east coast of North Island revealed a series of prominent, northeast trending ridges, one of which is Omakere Ridge. Here, a flare was observed during echosounder surveys of local fishermen in 1994 (Lewis and Marshall 1996, vent site number LM-9); dredging at this site failed to retrieve any seep-associated fauna. On side-scan sonar images obtained during SO191, five seep sites and one cold-water coral reef were found (Jones et al., this issue) based on their high backscatter intensity and

irregular form. The seep site Bear's Paw, and the cold-water reef Moa were visually studied and mapped by TV sled surveys (Jones et al., this issue). Sampling by TV-guided grab and coring recovered carbonate crusts, seep-associated fauna and gas hydrate at Bear's Paw (Jones et al., this issue) in 1100 m water depth (Fig. 1B). The carbonates as well as the transition zones between carbonates and sediments were densely populated by seep fauna like vestimentiferan polychaetes (*Lamellibrachia* sp.) and bivalve mollusk species (Thurber et al., this issue). In contrast to this almost exclusive chemoherm, the high relief carbonate outcrop at the Moa site was colonized in many places by cold-water corals (sampled with TV-grab at 1120 m water depth, Fig. 1D). Due to the absence of live chemosynthetic fauna, the main part of Moa is regarded as a relict seep site (Jones et al., this issue).

3. Sampling and analytical methods

3.1. Sampling of authigenic carbonates and surface sediments

Samples were obtained deploying the large video-guided grab (TVG) on board *RV SONNE* with a mouth opening of 1.8 m² and over 2 t closing pressure of the hydraulic system. Once the samples were recovered they were carefully inspected to document and sample their colonization by biological communities and their in-situ position at the sea floor.

The retrieved blocks, consisting of authigenic carbonates and consolidated sediment, were cut into sections by a specialized large scale disc saw (1.65 m in diameter). This technique provides continuous and fresh sampling surfaces throughout the centre of large blocks allowing new insights into internal structures/fabric, the precipitation processes, and the fluid channel systems.

3.2. Sub-sampling strategy and selection criteria

The sub-sampling focussed on aragonitic carbonate precipitates with discrete growth bands and fluid pathway structures, providing unaltered material for reliable isotope analyses. All sub-samples were taken with a mini-driller from freshly cut surfaces of solid precipitates, after discarding first drill steps as surface cleaning procedure. To secure the mineralogical composition as aragonitic (>98%), only samples were accepted that showed no calcite reflections in X-ray diffraction analyses.

Calcitic carbonates are less favoured for this kind of initial overview approach as their U–Th geochronology is affected by two disadvantageous facts. At first, they are potentially product of diagenetic recrystallisation of primary aragonitic precipitates. In this case, they do not necessarily reflect information about the original precipitation system solely. Secondly, even if defined as primary origin by detailed structural and mineralogical investigation, calcitic precipitates are often accompanied by low U and high Th contents. Both facts increase the required sample amount and complicate the correction for the isotopic composition of initial Th. Consequently, calcitic samples would lead to less lateral resolution in sub-sampling and less precise geochronology. The same assumption concerning sample amount, lateral and chronological precision is valid for isochron approaches, usually applied to circumvent the difficulties caused by high Th contents. Nevertheless, a good example for the potential and scope of U–Th dating approaches on a multiphase cold seep carbonate crust (Mg-calcite, calcite and aragonite) is presented by Bayon et al. (2009).

3.3. U–Th geochronology

This study is based on U–Th age data (Table 2) of little sample material in order to combine high structural resolution with the analytical precision of MC-ICP-MS (multi-collector-inductively coupled plasma-mass spectrometry). The U–Th isotope measurements were

Table 2

U–Th geochronology and light stable isotope signatures of authigenic carbonates and cold-water corals from cold seep sites at the Hikurangi Margin.

Site sample	Description	Sample weight (mg)	²³⁸ U conc. (µg/g)	²³² Th conc. (ng/g)	²³⁰ Th conc. (pg/g)	²³⁰ Th/ ²³² Th act. ratio	²³⁰ Th/ ²³⁴ U act. ratio	δ ²³⁴ U ₍₀₎ (‰)	δ ²³⁴ U _(T) (‰)	U–Th-ingrowth age (ka BP)	δ ¹³ C PDB of sample (‰)	δ ¹⁸ O PDB of sample (‰)
<i>Opouawe Bank/North Tower</i>												
138-1	Uppermost surface of the block	33.9	6.93 ± 0.03	168.0 ± 0.9	4.11 ± 0.02	4.60 ± 0.04	0.0264 ± 0.0017	146.6 ± 2.2	147.8 ± 2.2	2.92 ± 0.19	–46.20	3.37
138-2	Upper part of open pore system	19.0	5.78 ± 0.03	1.77 ± 0.01	2.64 ± 0.02	279.4 ± 2.9	0.0241 ± 0.0002	152.4 ± 2.0	153.5 ± 2.0	2.67 ± 0.03	–38.43	3.49
138-3	Intermediate of open pore system	17.3	7.76 ± 0.04	5.09 ± 0.04	3.37 ± 0.02	124.1 ± 1.3	0.0230 ± 0.0002	149.3 ± 2.5	150.4 ± 2.5	2.53 ± 0.02	–36.28	3.46
138-4	Lower part of open pore system	35.1	3.88 ± 0.02	25.78 ± 0.14	1.69 ± 0.01	12.3 ± 0.1	0.0217 ± 0.0004	149.9 ± 2.3	150.9 ± 2.3	2.39 ± 0.04	–39.39	3.54
138-5	Horizontal layer above sed. surface	9.5	5.66 ± 0.04	4.83 ± 0.04	3.81 ± 0.03	147.6 ± 1.7	0.0357 ± 0.0004	147.1 ± 1.7	148.7 ± 1.7	3.96 ± 0.05	–45.45	3.57
138-6	Solid rim beside sample 138-7	17.6	3.85 ± 0.02	0.79 ± 0.01	2.78 ± 0.02	662.2 ± 7.7	0.0383 ± 0.0003	150.6 ± 2.1	152.5 ± 2.2	4.26 ± 0.04	–46.47	3.50
138-7	Porous channel filling	15.7	14.5 ± 0.08	788.8 ± 5.0	11.42 ± 0.08	2.7 ± 0.03	0.0303 ± 0.0043	147.0 ± 2.6	148.4 ± 2.8	3.36 ± 0.48	–47.22	3.64
138-8	Intermediate vein system	19.0	4.12 ± 0.02	15.96 ± 0.11	3.04 ± 0.02	35.6 ± 0.4	0.0384 ± 0.0004	148.6 ± 2.4	150.4 ± 2.4	4.27 ± 0.05	–46.21	3.39
138-9	Solid rim of open pore space	17.7	3.29 ± 0.02	2.27 ± 0.02	2.40 ± 0.02	198.1 ± 2.0	0.0386 ± 0.0004	152.3 ± 2.1	154.2 ± 2.1	4.29 ± 0.04	–45.74	3.42
138-10	Vein system at base	34.5	5.13 ± 0.02	376.9 ± 2.0	5.77 ± 0.03	2.90 ± 0.02	0.0444 ± 0.0057	143.8 ± 2.1	145.8 ± 2.4	4.95 ± 0.65	–47.55	3.50
138-11	Dead solitary coral on top 138-1	2.9	2.68 ± 0.05	2.40 ± 0.04	0.12 ± 0.01	9.3 ± 0.6	0.0021 ± 0.0002	167.3 ± 5.1	167.4 ± 5.1	0.23 ± 0.02	–5.05	1.28
<i>Uruti Ridge/LM-10</i>												
316-1	Upper part of vertical vein	17.4	6.18 ± 0.03	2.99 ± 0.02	4.30 ± 0.03	269.6 ± 2.7	0.0371 ± 0.0003	144.0 ± 1.8	145.7 ± 1.8	4.12 ± 0.04	–52.00	3.03
316-2	Lower part of vertical vein	19.5	5.64 ± 0.03	3.04 ± 0.02	4.10 ± 0.03	252.3 ± 2.3	0.0387 ± 0.0003	143.4 ± 2.0	145.2 ± 2.0	4.31 ± 0.04	–51.16	3.02
316-3	Horizontal vein	9.5	5.03 ± 0.03	58.02 ± 0.43	10.31 ± 0.08	33.3 ± 0.4	0.1076 ± 0.0013	138.7 ± 2.2	143.6 ± 2.2	12.40 ± 0.16	–52.63	3.81
<i>Omakere Ridge/Bear's Paw</i>												
165-1	Rim of open pore space	38.2	2.34 ± 0.01	22.10 ± 0.12	1.03 ± 0.01	8.8 ± 0.1	0.0214 ± 0.0006	150.6 ± 2.4	151.6 ± 2.5	2.36 ± 0.07	–51.06	3.59
165-2	Porous channel filling	17.1	13.64 ± 0.07	1007.6 ± 5.9	8.90 ± 0.06	1.7 ± 0.0	0.0190 ± 0.0077	147.4 ± 2.1	148.3 ± 2.5	2.09 ± 0.85	–51.59	3.62
<i>Omakere Ridge/Moa</i>												
218-1	Coralline reef substrate	5.5	2.91 ± 0.06	39.94 ± 4.75	2.29 ± 0.03	10.8 ± 1.3	0.0395 ± 0.0012	134.3 ± 3.3	136.0 ± 3.4	4.39 ± 0.13	–7.14	–0.27
218-3	Dead solitary coral on 218-1	4.0	4.32 ± 0.02	5.73 ± 6.51	0.87 ± 0.02	28.4 ± 32.3	0.0105 ± 0.0004	134.5 ± 4.0	134.9 ± 4.0	1.16 ± 0.05	–3.89	1.51
227-1	Recent reef-forming coral	8.5	3.80 ± 0.03	–	0.095 ± 0.005	–	0.0013 ± 0.0002	146.3 ± 3.9	146.3 ± 3.9	0.15 ± 0.02	–	–

²³⁰Th/²³⁴U ratios and subsequently the calculated ages are corrected for potential detrital contribution applying a ²³⁰Th/²³²Th activity ratio of 0.75 ± 0.2, according to [Wedepohl \(1995\)](#). Note, in most cases this correction is negligible due to sufficiently high ²³⁰Th/²³²Th activity ratios in the carbonates. Nevertheless, despite precise isotope measurements, for some samples enlarged age uncertainty must be deduced. Lacking or in italics given Th data correspond to measurements on ²³²Th amounts below or close to the detection limit. The age of sample 227-1 displays the theoretical equivalent of the primary ²³⁰Th/²³⁴U activity ratio in this recent coral. The δ²³⁴U₍₀₎ value represents the originally today measured (²³⁴U/²³⁸U) activity ratio, given in delta notation (δ²³⁴U₍₀₎ = ((²³⁴U_{act}/²³⁸U_{act}) – 1) · 1000). Displayed δ²³⁴U_(T) values reflect age corrected (²³⁴U/²³⁸U) activity ratios by recalculating the decay of ²³⁴U for the time interval T (δ²³⁴U_(T) = δ²³⁴U₍₀₎ · exp(λ₂₃₄ · T)), determined from ²³⁰Th/²³⁴U age of each individual sample. Note, due to young ages of this sample set, the impact of age correction on the interpretation of δ²³⁴U values is almost negligible. All errors are deduced on 2 σ level. δ¹³C and δ¹⁸O values are referred in ‰ to the PDB scale. Counting statistics of each sample measurement was below the representative standard deviation of 17 accompanying standard measurements (0.028% for δ¹³C, 0.039% for δ¹⁸O).

performed on a VG Elemental AXIOM MC-ICP-MS at IFM-GEOMAR applying the multi-static MIC (multi-ion-counting)-ICP-MS approach after Fietzke et al. (2005). For isotope dilution measurements a combined $^{233}\text{Th}/^{236}\text{U}/^{229}\text{Th}$ -spike was used, with stock solutions calibrated for concentration using NIST-SRM 3164 (U) and NIST-SRM 3159 (Th) as combi-spike calibrated against CRM-145 uranium standard solution (also known as NBL-112A) for U-isotope composition, and against a secular equilibrium standard (HU-1, uranium ore solution) for determination of $^{230}\text{Th}/^{234}\text{U}$ activity ratio. Whole procedure blank values of this sample set were measured around 0.1 fg for ^{230}Th , around 2 pg for ^{232}Th and between 2 and 5 pg for U, which are in the typical range of this method and laboratory. Element separation procedure was based on Eichrom-UTEVA resin. Calculation of geochronological data and activity ratios is based on the decay constants given by Cheng et al. (2000).

Each set of element separation was accompanied by runs of aliquots of the HU-1 equilibrium standard solution to verify procedure reproducibility. A methodology depending uncertainty of less than 0.5% on $^{230}\text{Th}/^{234}\text{U}$ activity ratios was reached; the geochronological uncertainties given in Table 2 are dominated by the analytical error of individual sample measurement. The applied data reduction includes a correction for isotopic composition of incorporated Th of detrital origin, according to continental crust values (Wedepohl, 1995) as approximation for involved shelf sediments (details given in Table 2). Due to the selection strategy for the majority of the sub-samples this correction is almost negligible. An additional, more exact determination of potentially deviating isotope signatures of dissolved Th in the precipitation feeding cold seep fluid is hampered by the lack of adequate fluid sample material. An alternative, analytically sophisticated and site-specific approach for Th corrections is presented by Bayon et al. (2009) that also works for cold seep carbonates with high Th content. According to published cold seep U–Th data (e.g. Teichert et al., 2003) the $^{234}\text{U}/^{238}\text{U}$ ratios are presented in $\delta^{234}\text{U}$ notation (details given in Table 2).

3.4. C and O isotope analyses

In order to identify the methane seep relation of carbonates detailed $\delta^{13}\text{C}$ and $\delta^{18}\text{O}$ analyses are crucial requirements. A correlation of light stable isotope signatures with age constrains (Fig. 3) and local habitat characteristics may reflect the impact of varying vent activity through time and contributes to over-regional comparison of seep settings. Stable oxygen and carbon isotope measurements were carried out at the isotope laboratory at IFM-GEOMAR with a CARBO KIEL automated carbonate preparation devices linked on-line to a FINNIGAN MAT 252 mass spectrometer. External reproducibility was 0.028‰ for $\delta^{13}\text{C}$ and 0.039‰ for $\delta^{18}\text{O}$ (1-sigma values), as calculated from 17 replicate analyses of the internal carbonate standard (Solnhofen Limestone) performed before and after the analyses of our carbonate samples. The isotope data are referred to the PDB scale.

4. Sample description and site-specific results

During various tracks using the video sled OFOS (Ocean Floor Observation System) different types of cold seep carbonates were

observed during cruise SO191. Most abundant were carbonates forming flat pavements at the sediment seawater interface. These carbonates were different from large brownish to blackish blocks characterized by a smooth and even surface not showing any remarkable biological colonization. Another type of light brown to white carbonate reached upward into the bottom water column and was marked by a porous and brecciated surface structure (chemoherm).

In an attempt to characterize different cold seep settings, results combined from structural, mineralogical, and isotope geochemical analysis (Table 2, Fig. 3) are presented in geographical order from South to North, facilitating their comparison along the Hikurangi Margin.

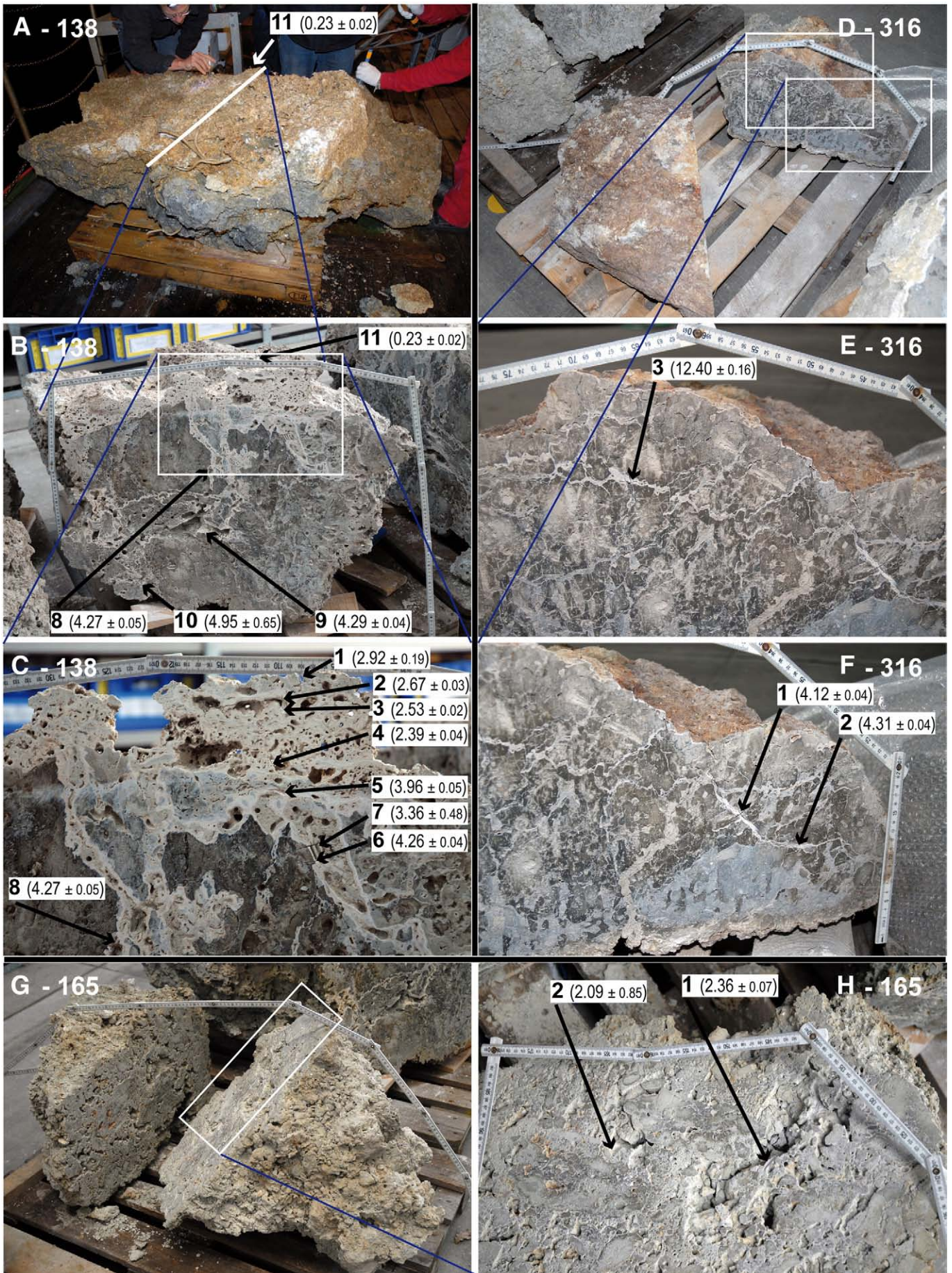
4.1. Opouawe Bank

On the Opouawe Bank the largest carbonate sample (weight approx. 2.5 t) was obtained from the North Tower site (Table 1 #138, Fig. 1F, G). Visual inspection revealed sessile seep fauna like vestimentiferan polychaetes (*Lamellibrachia* sp.) with tubes extending in the fluid channel system of the large carbonate block (Fig. 2A). Those parts of the block, which were exposed to the bottom water current regime, were colonized by solitary cold-water corals (*Caryophyllia* sp., *Desmophyllum dianthus*).

The large vertical cross-cut (Fig. 2B) provides insight into the fine structured, upwards branching fluid channel system within, and a porous layer of carbonate precipitate on top of the consolidated sediment. Within the fluid channel system, open pore space (e.g. sub-sampling spot 138-9, Fig. 2B) can be observed and the wider the channel system the thicker and more porous are the stable and rim-like cements on the sediment/channel-interface. The U–Th age profile through the fluid pathway and vein system of the block revealed two major phases of vent activity according to distinct $\delta^{13}\text{C}$ signatures (Fig. 3).

Following the fluid path from the bottom (Fig. 2B, spot 138-10) to a rather thin, but solid layer on top of the sediment surface (Fig. 2C, spot 138-5) our analyses reveal a succession from 4950 ± 650 to 3960 ± 50 years BP. The prior reflects the influence of increased Th concentration on U–Th age precision, but gives a first estimate for the timing of initial precipitation. This phase is characterized by a $\delta^{234}\text{U}_{(T)}$ value of $145.8 \pm 2.4\%$, which is according to Henderson and Anderson (2003) identical with the modern seawater signature ($146 \pm 2\%$). More precisely dated intermediated profile steps represent ages of 4290 ± 40 (Fig. 2B, spot 138-9) and 4270 ± 50 (Fig. 2B, spot 138-8) years BP and point with $\delta^{234}\text{U}_{(T)}$ values of 154.2 ± 2.1 and $150.4 \pm 2.4\%$, respectively, to an increasing and varying impact of a more reducing fluid environment (Teichert et al., 2003). The porous and structurally weak fluid channel filling at spot 138-7 (Fig. 2C) shows an age of 3360 years BP, with increased uncertainty of ± 480 years due to incorporation of higher Th levels. Remarkable is the combination of the highest observed U concentration (14.5 ppm) with a $\delta^{234}\text{U}_{(T)}$ value ($148.4 \pm 2.8\%$) again close to modern seawater. In contrast, the massive rim at spot 138-6 directly aside (Fig. 2C, 4260 ± 40 years BP) represents the fluid channel stabilizing pre-cursor precipitate with only 3.85 ppm U at slightly elevated $\delta^{234}\text{U}_{(T)}$ signature of $152.5 \pm 2.2\%$. Note, all these vein and fluid channel precipitates are very similar in $\delta^{13}\text{C}$ signature, covering a narrow range between -47.55 and -45.45% (Fig. 3).

Fig. 2. Internal precipitation structures and sub-sampling spots on surfaces of large cross-cuts through blocks of calcified sediments from Hikurangi Margin, recovered with TV-guided grab during cruise SO191 (U–Th ages given in ka BP). For scale please refer to displayed cruise participants and 20 cm length for each section of the folding rule. Spots of sub-samples are marked with arrows and succession of single numbers on each cross-cut for identification in Table 2. A–C: Largest recovered block from North Tower site of Opouawe Bank (station # 138). A: In full extension during surface sampling by biologists on deck of RV SONNE, displaying brown to whitish layers on top of solid sediment. B: Overview of vertical cross-cut showing upward widening vein and channel system with still open pore volume, surrounded by densely calcified sediment (white square corresponds to C). C: Enlargement documents the structural change of carbonate type from vein structures over stable open channels and their filling to precipitates above the sediment. D–F: Most dense calcified sediment sample of this study from the top of Uruti Ridge close to the LM-10 site (station # 316). D: Overview displaying massive and closed structure of the block with a fine distributed vein system, white squares mark positions of enlargements E and F. E: Details of the uppermost left part with dominant horizontal veins. F: Details of upward widening vein system in lower right part. G and H: Least mature calcified sediment, rich in remnants of cold seep fauna, from Bear's Paw of Omakere Ridge (station # 165). G: Overview reflecting typical block size, low density and pronounced content of shell fragments. Solid vein structures are hardly identifiable. H: Close-up of open channel and pore volume structures within a rather diffuse calcified matrix, displaying challenging sample situation for recovery of distinct growth of aragonitic composition. (For interpretation of the references to colour in this figure legend, the reader is referred to the web version of this article.)



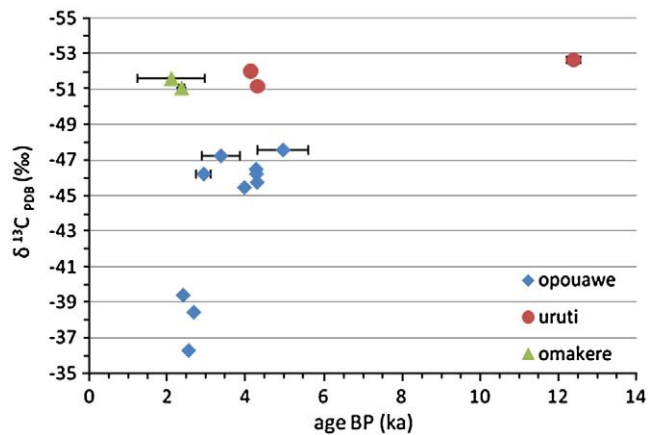


Fig. 3. $\delta^{13}\text{C}_{\text{PDB}}$ (‰) and U–Th ages in thousand years before present (ka BP) from three different cold seep areas of the Hikurangi Margin (Opuawe Bank = diamonds, Uruti Ridge = dots, Omakere Ridge = triangles).

Comparable with the channel filling sample (Fig. 2C, spot 138-7) the data of the uppermost surface of the block (Fig. 2C, spot 138-1) revealed an age of 2920 ± 190 years BP. The increased Th content introduced an enlarged age uncertainty, related to the precipitation of this layer at ongoing exposure to the particle fall-out of the bottom water column. Characteristically, this precipitation is accompanied by a $\delta^{234}\text{U}_{(T)}$ signature ($147.8 \pm 2.2\%$) close to modern seawater and a clear methane influence as shown by a $\delta^{13}\text{C}$ signature of -46.2% .

Another group of sub-samples shows distinctively heavier $\delta^{13}\text{C}$ signatures of -39.39 to -36.28% . The related age data cover a rather narrow range from 2670 ± 30 (Fig. 2C, spot 138-2) to 2530 ± 20 (Fig. 2C, spot 138-3) and 2390 ± 40 (Fig. 2C, spot 138-4) years BP. The sample positions reflect a downward succession of the precipitation within the open pore space, from the uppermost chemoherm surface towards the sediment body at slightly elevated $\delta^{234}\text{U}_{(T)}$ values between 153.5 ± 2 and $150.4 \pm 2.5\%$. The $\delta^{18}\text{O}$ signatures of all sub-samples cluster between 3.37 and 3.64‰ without clear correlation to the observed $\delta^{13}\text{C}$ systematic.

U–Th dating of a dead solitary cold-water coral on top of the block revealed an age of 230 ± 20 years BP (Fig. 2A, spot 138-11) for a late stage of coral settling. The coral has a $\delta^{13}\text{C}$ signature of -5.05% and an unexpected high $\delta^{234}\text{U}_{(T)}$ value ($167.4 \pm 5.1\%$).

4.2. Uruti Ridge

The long video survey during the search for a sampling opportunity with the TVG on top of LM-10 at Uruti Ridge showed a solid carbonate pavement of the sea floor with large lateral extend (Fig. 1E). Fractures in the carbonate platform were colonized by vestimentiferan tubeworms (*Lamellibrachia* sp.). Finally, a representative sample was recovered from this pavement in 756 m water depth (Table 1, #316) close to the original LM-10 position (Lewis and Marshall, 1996). The compact brownish block can be described as a dense and solid calcified sediment with a disperse vein system representing a mature calcification stage (Fig. 2D). U–Th age dating of sub-samples from the cross-cut represents at least two generations of vent activity and related precipitation of the fluid vein system. A horizontal vein in the upper left part of the cross-cut (Fig. 2E, spot 316-3) showed the oldest U–Th age ($12,400 \pm 160$ years BP), the lightest $\delta^{13}\text{C}$ ($-52.63 \pm 3.81\%$) and heaviest $\delta^{18}\text{O}$ signatures (3.81‰) in this study. A significant younger phase could be detected by dating the lower (Fig. 2F, spot 316-2) and upper part (Fig. 2F, spot 316-1) of a vein, tending oblique vertical to the first. The age data of 4310 ± 40 (spot 316-2) and 4120 ± 40 years BP (spot 316-1) are very close but not overlapping within error, therefore, reflecting a successive upward precipitation trend and closing of the vein system. Note, the growth

systematic and age range of this generation is similar to observations on the vein and channel system at the North Tower site of Opuawe Bank. Despite the rather large time gap, both observed phases of the Uruti sample cover only a very narrow range of less than 2‰ in $\delta^{13}\text{C}$ from -52.63 to -51.16% , which is distinctively different to the North Tower site. Their $\delta^{234}\text{U}_{(T)}$ values are within error overlapping between $143.6 \pm 2.2\%$ (spot 316-3) and $145.7 \pm 1.8\%$ (spot 316-1), the latter is almost identical to modern seawater. Inverse to the early phase (spot 316-3) the younger generation shows (Fig. 3) the lightest $\delta^{18}\text{O}$ signatures of this study (3.02‰).

4.3. Omakere Ridge

4.3.1. Bear's Paw

The video transects with OFOS and the TVG showed remnants of cold seep fauna associated to rounded boulder structures with vestimentiferan tubeworms (*Lamellibrachia* sp.) extending from fractures and channels into the bottom water (Fig. 1B). Carbonate samples (Table 1, #165) obtained from the Omakere Ridge (Fig. 1C) represent calcified sediment of low maturity and a less pronounced to rare aragonite precipitation (Fig. 2G). U–Th age data reflect the youngest phase of authigenic carbonate precipitation determined for Hikurangi Margin cold seep sites in this study. In the cross-cut sub-samples a solid, almost transparent coating inside an open pore space (Fig. 2H, spot 165-1) revealed an age of 2360 ± 70 years BP. Only one other spot could be sampled fulfilling the aragonite requirement and representing less dense pore volume precipitation processes (Fig. 2H, spot 165-2). The deduced age of 2090 years BP points to an expected slightly younger phase of precipitation within the fluid channel, but, due to typically increased Th content (highest in this study, second highest content in U) an uncertainty of ± 850 years does not allow a geochronological separation. Regardless this uncertainty, a general young age range is indicated which is identical to the late stage precipitation at the Opuawe Bank.

$\delta^{13}\text{C}$ signatures of -51.06% (rim, spot 165-1) and -51.59% (channel, spot 165-2) are similar to the findings at Uruti Ridge, whereas the $\delta^{18}\text{O}$ values of 3.59‰ and 3.62‰ correspond to the Opuawe Bank data. In contrast to the narrow range in $\delta^{13}\text{C}$ and $\delta^{18}\text{O}$ for both structurally quiet different precipitation types (Fig. 2H, spot 165-1 and -2), the $\delta^{234}\text{U}_{(T)}$ and $\delta^{13}\text{C}$ value tends to be higher in the solid vein- or rim-like precipitate ($151.6 \pm 2.5\%$, spot 165-1), when compared to the porous channel filling precipitate ($148.3 \pm 2.5\%$, spot 165-2). Although these $\delta^{234}\text{U}_{(T)}$ values are showing some overlap in error the correlation trend with $\delta^{13}\text{C}$ fits to observations in the Opuawe Ridge data set between rim (Fig. 2C, spot 138-6) and channel filling precipitate (Fig. 2C, spot 138-7).

4.3.2. Moa

The Moa site was selected in order to recover reef-forming corals together with the cold seep related hard substrate underneath (Table 1, # 218). In contrast to the other sampling sites of this study, the high relief carbonate outcrop at Moa was colonized in many spots by reef-forming and solitary cold-water corals. Deploying the TV-grab in 1107 to 1120 m water depth (Fig. 1D) fossil and living coral specimens (Table 1, # 227) were sampled. Unfortunately, the seafloor underneath the coral reef could not be penetrated successfully for recovering underlying authigenic cold seep carbonates. This would have been useful to study the temporal relation of seep activity and coral reef formation. Nevertheless, due to its prominent structure and obvious multi-phase colonization this cold-water coral reef provides an isotope geochemical and geochronological reference site for coral colonisation of cold seep carbonate along the Hikurangi Margin.

This initial U–Th geochronology approach at Moa addresses the timing of solitary cold-water coral settling on fossil coralline reef substrate. U–Th data of the fossil reef (Table 2, 218-1) lead to an age of 4390 ± 130 years BP, resulting in a $\delta^{234}\text{U}_{(T)}$ value ($136.0 \pm 3.4\%$)

slightly lower than modern seawater. This is accompanied by a rather light $\delta^{13}\text{C}$ signature of -7.14‰ . In contrast, one solitary coral (*Desmophyllum dianthus*; Table 2, 218–3), settled directly on sample 218-1, gives an age of 1160 ± 50 years BP. This sample reveals a similar $\delta^{234}\text{U}_{(T)}$ value ($134.9 \pm 3.4\text{‰}$) and a heavier $\delta^{13}\text{C}$ signature of -3.89‰ .

In order to obtain the initial isotope composition, the uppermost part of a living reef-forming coral (*Solenosmilia variabilis*; Table 2, 227-1) from the second Moa site was analysed (Table 1, #227, Fig. 1D). This juvenile fragment revealed a modern seawater matching $\delta^{234}\text{U}_{(0)}$ value of $146.3 \pm 3.9\text{‰}$ and an initial $^{230}\text{Th}/^{234}\text{U}$ activity ratio of 0.0013 ± 0.0002 , corresponding to a theoretical age of 150 years BP. Due to high growth rates of reef-forming corals (Roberts et al., 2009) the integration of some years of precipitation within the mini-drill based sub-sampling is negligible for any age correction.

5. Discussion

5.1. Timing of cold seep activity and potential driving processes

The obtained age data set reflects very close similarities between the southernmost (Opouawe Bank/North Tower) and the northernmost (Omakere Ridge/Bear's Paw) site of this study. They represent the latest stage of cold seep related carbonate precipitation at around 2390 ± 40 , 2360 ± 70 and 2090 ± 850 years BP. Both sites are in the same water depth between 1050 and 1100 m. In contrast, the oldest age of near surface vein precipitates was analysed to be $12,400 \pm 160$ years BP at Uruti Ridge which is the shallowest sampling site of the study (750 m water depth). This site was at least active up to 4120 ± 40 years BP. This implies a short time interval of contemporaneous activity around 4300 years (s. Table 2) during the late stages of seepage at Uruti Ridge and the beginning at Opouawe Bank (oldest age determined: 4950 ± 650 years BP). The significance of the detected age succession and site-specific age range is supported by a strong correlation with gradual changes of sediment solidification due to cold seep related calcification processes. This impact of cold seep activity seems to be least pronounced at Omakere Ridge (Bear's Paw, youngest age and shortest activity period, Fig. 2G–H) when compared to samples from the Uruti Ridge (longest time interval of activity, Fig. 2D–F) and Opouawe Bank (Fig. 2B–C).

As a first approximation, these findings imply younger seep activity towards larger water depth. On the other hand, sites which have been active in earlier phases may have been shifted and influenced by pro-grading uplift and the compressional tectonic regime of the accretionary margin. Depending on the position within the ridge structure, compression might block existing fluid pathways and creates new seep sites on the ridge flanks. However, the data base needs to be extended significantly for more robust interpretations of systematic changes in distribution of active vent sites at the Hikurangi Margin.

In comparison to other age data of cold seep paleoactivity within the circum-Pacific framework, e.g. published by Teichert et al. (2003; accretionary prism, Hydrate Ridge, Cascadia Margin, off Oregon) and Kutterolf et al. (2008; erosive subduction system, Central American forearc, off Nicaragua and Costa Rica), the presented Hikurangi Margin data reflect a rather short interval from the Younger Dryas on only. This time span does not allow a direct contribution to the ongoing discussion concerning long-term correlation of major cold seep activity phases with periods of fast sea-level changes and low stands. The latter scenario suggests hydraulic pressure influenced intensification of fluid flow at cold seeps. On much shorter time scales this process has been observed for tidally controlled fluctuations. High rates of fluid flow were measured at low tides whereas high tides were characterized by low rates of fluid flow (LaBonte et al., 2007; Linke et al., this issue). This principle of tidal pumping is driven by changes of the balance between static hydraulic head of the water

column and the dynamic hydraulic pressure of the fluid emanating pore water and cold seep system (Liebetrau et al., 2008). Applied on geological time scales the hydraulic head is mainly depending on the global influences of major sea-level changes, whereas the fluid pressure and availability as well as the emplacement of fluid pathways is rather controlled by local to regional tectonic changes (Kutterolf et al., 2008). Additionally, sea floor hydrologic systems respond to episodic events such as tsunamis, gas discharge, and seismic and aseismic strain (e.g. Brown et al., 2005; Ge and Screaton, 2005; Mau et al., 2007; Tryon et al., 2002).

Seismic strain may be of great importance for cold seep settings at the tectonically highly active Hikurangi Margin, which is characterized by an active oblique subduction and build-up of accretionary ridges. Within the central part of the Northern Island of New Zealand the Taupo Volcanic Zone (TVZ) represents an active back arc extension area (Peltier et al., 2009) parallel to the Hikurangi Margin. The most recent major eruption took place about 1830 years ago on a NE–SW-trending fissure at Lake Taupo (Wilson et al., 1995), close to the investigated cold seep sites of this study. Therefore, the youngest phase of carbonate precipitating cold seep activity identified at Omakere Ridge (Bear's Paw, Table 2) could be a late stage marine precursor of major changes within the regional tectonic framework.

5.2. Varying cold seep activity monitored by precipitates within the fluid pathway

Age data of the sample profile from Opouawe Bank start around 5000 years BP with a primary upward progressing precipitation that implies a potential drop in intensity of fluid flux in a time interval from around 4000 to 3000 years BP. This drop in flux activity is characterized by lowering $\delta^{234}\text{U}_{(T)}$ values close to modern seawater within the open fluid channel system, indicating decreased fluid advection rates.

In our study, the related less dense to porous precipitates within the open channel systems at Omakere Ridge and Opouawe Bank are characterized by lighter $\delta^{13}\text{C}$ signatures and significant enrichment in U and Th, relative to the more solid vein- or rim-like precipitates. Such a significant increase of Th in the carbonate phase is generally related to enhanced incorporation of particles during precipitation. Due to its preferential uptake of U organic matter can be assumed as important particle source. The trend to lighter $\delta^{13}\text{C}$ values points to a stronger impact of methane related instead of water column derived matter. These observations suggest precipitation of the porous carbonates during times of less vigorous methane emanation. Such phases may have been accompanied by an increased incorporation of organic particles that partly derived from AOM consortia, according to observations of heterogeneous biomarker distributions in carbonate phases at Hydrate Ridge (Leefmann et al., 2008). The data and observed structures indicate a later stage for the channel filling precipitation.

5.3. Comparison of C and O isotope signatures

The comparison of the light stable isotope values in this study shows rather similar $\delta^{13}\text{C}$ signatures of around -52‰ at Uruti and Omakere Ridge, almost age independent. The North Tower sample (Opouawe Bank) reflects site-specific heavier signatures in two distinct clusters at around -47‰ and -38‰ . The first cluster signature is restricted on vein filling precipitates within the sediment, the layer directly above the sediment body (Fig. 1C, spot 138-5) and the uppermost chemoherm layer on top of the sampled block (Fig. 1C, spot 138-1). This similarity implies a comparable fluid flux and source signature, despite obvious differences in growth structure, precipitation process and timing of emplacement. The second cluster of $\delta^{13}\text{C}$ values (-38‰) is restricted to the youngest precipitates, filling the open pore space of

chemoherm build-ups above the sediment surface. This indicates a relative decrease in fluid flux in the late stage of seep activity. In contrast to $\delta^{13}\text{C}$, the $\delta^{18}\text{O}$ data (Table 2) of cold seep carbonates from Opouawe Bank and Omakere Ridge cluster in a very narrow range between 3.35 and 3.65‰ only. Whereas the widest range in $\delta^{18}\text{O}$ is covered within the sample from Uruti Ridge (3 to 3.8‰), accompanied by the largest time span of seep activity at rather constant $\delta^{13}\text{C}$ values. The trend of heavier $\delta^{18}\text{O}$ at the oldest age (around 12,400 years BP) and lighter values at younger ages correlates to the seawater evolution described for this region by Elderfield et al. (2009). Accordingly, our data set implies rather decoupled trends, with $\delta^{13}\text{C}$ values dominated by site-specific influences of methane sources and $\delta^{18}\text{O}$ values appearing to be sensitive for changes in bottom water temperatures (Han et al., 2008).

5.4. Relation of cold-water coral colonization and cold seep activity

Seafloor observations during SO191 indicated massive authigenic carbonates as the pre-dominant substrate for cold-water coral colonization and reef formation. The first coral age constrain from Opouawe Bank (230 ± 20 years BP) represents a late stage of solitary coral settling, reflecting a time gap to the formation of underlying cold seep carbonates of at least 2000 years. No direct coupling with cold seep activity is implied. Due to the detected time gap no direct comparison of the two potential archives for enhanced fluid flux (cold seep carbonates) and its impact on the bottom water chemistry (corals) is provided. Accordingly, the rather heavy $\delta^{13}\text{C}$ signature (-5.05% , 138–11) of this young coral seems to be not monitoring a significant enrichment of lighter methane related carbon in the bottom water column. In contrast, the accompanying unexpected high $\delta^{234}\text{U}_{(T)}$ value ($167.4 \pm 5.1\%$) could be interpreted as incorporation of fluid or pore water signatures. This coral value is even higher than all findings in this study for precipitates directly within the fluid pathway, although these fluid pathways were exposed to the highest potential impact of elevated $\delta^{234}\text{U}$ fluid signatures. Combined with the age data and $\delta^{13}\text{C}$ evidences against contemporaneous enhancement of fluid flux, this high $\delta^{234}\text{U}_{(T)}$ coral value is most probably related to a secondary impact of early diagenesis as discussed by Ponse-Branchu et al. (2005). The calculated age is regarded as a minimum age and is topic of ongoing coral specific analyses at this site. In any case the result implies a passive support of coral settling by cold seep activity, just providing hard substrate and exposure to a high current regime with low to negative sedimentation rate.

In contrast, first results on reef geochronology at Omakere Ridge (Moa site) suggest a major reef formation around 4400 years BP, accompanied by a rather light $\delta^{13}\text{C}$ signature of -7.14% . Most probably, this phase of coral settling is closely related to a regional phase of intensified cold seep carbonate precipitation and sediment solidification between 5000 and 4000 years BP that occurred along the entire Hikurangi Margin. Taking into account that carbonates affected by cold seep fluid flux would rather deviate from modern seawater towards elevated $\delta^{234}\text{U}_{(T)}$ values (Teichert et al., 2003), the observed lower $\delta^{234}\text{U}_{(T)}$ of the fossil coral material at Moa implies a secondary relative loss of ^{234}U . Thus the related coral age data should be regarded as maximum estimates.

Due to the general absence of live chemosynthetic cold seep fauna, the main part of Moa is regarded as a relict seep site (Jones et al., this issue). This assumption is supported by rather heavy $\delta^{13}\text{C}$ signature (-3.89%) of a solitary coral grown in a later stage (1160 ± 50 years BP) on the fossil reef. Additionally, a minimum time gap of approximately 2000 years between the latest known stage of pre-dominant authigenic carbonate precipitation (Table 2) and the observed living reef-forming colonies exists (Fig. 1D, Table 2). Therefore, the findings at Moa support the assumption that cold seep activity is a major pre-requisite for providing suitable, long

lasting and exposed hard substrate; active seepage is not required for successful coral growth.

In this context of an inactive seep site, the U–Th data of a recent reef-forming cold-water coral (*Solenosmilia variabilis*, Moa, 227–1) provided approximative values for the initial $^{230}\text{Th}/^{234}\text{U}$ activity ratio (0.0013 ± 0.0002) and $\delta^{234}\text{U}_{(0)}$ signature ($146.3 \pm 3.9\%$). Contributing to the isotope geochemical comparison of cold-water coral environments, these data reflect growth conditions and seawater values within the bottom water (1120 m depth) at low to not detectable cold seep activity.

6. Conclusion and perspective

In this study we focused on the geochemical, mineralogical and structural analyses of authigenic carbonate samples recovered from Opouawe Bank, Uruti and Omakere Ridge. Aragonite precipitates from these three cold seep areas at Hikurangi Margin reflect different generations of seep activity between $12,400 \pm 160$ and 2090 ± 850 years BP.

The youngest stage was identified as contemporaneous intensified cold seep activity at the southernmost and northernmost sampling sites, sharing the same water depth (1050 to 1100 m), implying margin-wide tectonic or hydrological changes as driving process.

An intermediate phase of carbonate precipitation, establishing vein and channel structures within the sediment body, can be deduced for a time interval between 4950 ± 650 and 3960 ± 50 years BP. Within this period a stage of intensified focused seep activity was detected at Uruti Ridge and Opouawe Bank at around 4300 years BP.

$\delta^{13}\text{C}_{\text{PDB}}$ data reflect site and carbonate type specific signatures, clustering around -52% (Uruti and Omakere Ridge) and -47% for the fluid pathway system and the uppermost part of the block recovered at North Tower site (Opouawe Bank). The latter site also shows a cluster around -38% for late stage precipitates in the chemoherm cavities above the sediment.

Porous aragonites within the open fluid channel system reflect a trend of decreasing $\delta^{234}\text{U}_{(T)}$ values down to signatures close to modern seawater, accompanied by increasing concentrations of Th and U and a trend towards lighter $\delta^{13}\text{C}_{\text{PDB}}$ signatures. Combining these observations, assigns those precipitates to phases of less vigorous fluid seepage and increased incorporation of particles that may partly derived from AOM consortia. The latter working hypothesis requires further verification by biomarker studies.

The observed cold-water corals seem to depend on the occurrence of authigenic carbonates like chemoherm or calcified sediments and their long-term exposure to strong bottom currents. Seafloor observations combined with preliminary age data indicate a significant time gap of up to 2000 years between cold seep activity and first colonization. In order to contribute to the reconstruction of long-term variation of seep activity and the potential influences of glacial and interglacial cycles an additional sampling campaign is required, providing deeper carbonate units that can only be recovered by submarine rock drill tools.

Acknowledgements

We are grateful for the support of chief mate Lutz Mallon, officers and crew of RV SONNE during cruise SO191. This is publication Geotech-1288. Cruise SO191 was part of the COMET project in the framework of the R&D program GEOTECHNOLOGIEN, both funded by the German Ministry of Education and Research (Grant No: 03G0600D and 03G0191A). Dr. J. Fietzke is especially acknowledged for maintaining the Axiom MC-ICP-MS on high performance for the U–Th measurements, Dr. A. Rüggeberg for supporting the cold-water coral work, A. Kolevica as well as D. Mikschl for clean-lab support, J. Heinze for XRD measurements on smallest sample amounts and L. Haxhij for

performing stable isotope measurements. Volker Thiel, an anonymous reviewer and the editor are acknowledged for providing thoughtful and constructive reviews and comments, which improved significantly our manuscript.

References

- Aloisi, G., Bouloubassi, I., Heijs, S.K., Pancost, R.D., Pierre, C., Sinninghe Damsté, J.S., Gottschal, J.C., Forney, L.J., Rouchy, J.-M., 2002. CH₄-consuming microorganisms and the formation of carbonate crusts at cold seeps. *Earth Planet. Sci. Lett.* 203, 195–203.
- Baco, A.R., Rowden, A.A., Levin, L.A., Smith, C.R., Bowden, D., RENEWZ I cruise scientific party, this issue. Initial characterization of cold seep faunal communities on the New Zealand margin. *Mar. Geol.* doi:10.1016/j.margeo.2009.06.15
- Barnes, P.M., Lamarche, G., Bialas, J., Henrys, S., Pecher, I., Netzeband, G.L., Greinert, J., Mountjoy, J.J., Pedley, K., Cruttschley, G., this issue. Tectonic and geological framework for gas hydrates and cold seeps on the Hikurangi subduction margin, New Zealand. *Mar. Geol.* doi:10.1016/j.margeo.2009.03.12.
- Bayon, G., Henderson, G.M., Bohn, M., 2009. U–Th stratigraphy of a cold seep carbonate crust. *Chem. Geol.* 260, 47–56, doi:10.1016/j.chemgeo.2008.11.020.
- Becker, E.L., Cordes, E.E., Macko, S.A., Fisher, C.R., 2009. Importance of seep primary production to *Lophelia pertusa* and associated fauna in the Gulf of Mexico. *Deep-Sea Res.* 56, 786–800.
- Bialas, J., Greinert, J., Linke, P., Pfannkuche, O., 2007. FS Sonne Fahrtbericht/Cruise Report SO 191 New Vents. IFM-GEOMAR, Leibniz-Institut für Meereswissenschaften, Kiel, Germany. 190 pp.
- Boetius, A., Ravensschlag, K., Schubert, C.J., Rickert, D., Widdel, F., Gieskes, A., R., Amann, Jørgensen, B.B., Witte, U., Pfannkuche, O., 2000. A microbial consortium apparently mediating anaerobic oxidation of methane. *Nature* 407, 623–626.
- Brown, K.M., Tryon, M.D., DeShon, H.R., Dorman, L.M., Schwartz, S.Y., 2005. Correlated transient fluid pulsing and seismic tremor in the Costa Rica subduction zone. *Earth Planet. Sci. Lett.* 238, 189–203.
- Campbell, K.A., 2006. Hydrocarbon seep and hydrothermal vent paleoenvironments and paleontology: past developments and future research directions. *Palaeogeogr., Palaeoclimat., Palaeoecol.* 232, 362–407.
- Campbell, K.A., Farmer, J.D., Des Marais, D., 2002. Ancient hydrocarbon seeps from the Mesozoic convergent margin of California: carbonate geochemistry, fluids and paleoenvironments. *Geofluids* 2, 63–94.
- Campbell, K.A., Francis, D.A., Collins, M., Gregory, M.R., Nelson, C.S., Greinert, J., Aharon, P., 2008. Hydrocarbon seep-carbonates of a Miocene forearc (East Coast Basin), North Island, New Zealand. *Sediment. Geol.* 204, 83–105.
- Campbell, K.A., Nelson, C.S., Alfaro, A.C., Boyd, S., Greinert, J., Nymann, S.L., Grosjean, E., Logan, G.A., Gregory, M.R., Cooke, S., Linke, P., Milloy, S., Wallis, I., this issue. Geological imprint of methane seepage on the seabed and biota of the convergent Hikurangi Margin, New Zealand: Survey of core and grab samples. *Mar. Geol.* doi:10.1016/j.margeo.2010.01.002.
- Cheng, H., Edwards, R.L., Hoff, J., Gallup, C.D., Richards, D.A., Asmerom, Y., 2000. The half-lives of uranium-234 and thorium-230. *Chem. Geol.* 169, 17–33.
- Elderfield, H., Greaves, M., Barker, S., Hall, I.R., Tripathi, A., Ferretti, P., Crowhurst, S., Booth, L., Daunt, C., 2009. A record of bottom water temperature and seawater $\delta^{18}\text{O}$ for the Southern Ocean over the past 440 kyr based on Mg/Ca of benthic foraminifera *Uvigerina* spp. *Quaternary Science Reviews*, in press. doi:10.1016/j.quascirev.2009.07.013.
- Fietzke, J., Liebetrau, V., Eisenhauer, A., Dullo, W.-C.H., 2005. Determination of Uranium isotope ratios by multi-static MIC-ICP-MS: method and implementation for precise U- and Th-series isotope measurements. *J. Anal. Atom. Spectrom.* 20, 395–401.
- Ge, S., Sreanator, E., 2005. Modeling seismically induced deformation and fluid flow in the Nankai subduction zone. *Geophys. Res. Lett.* 32, L17301, doi:10.1029/2005GL023473.
- Greinert, J., Lewis, K., Suess, E., Pecher, I., Rowden, A., De Batist, M., Linke, P., Bialas, J., this issue. Methane seepage along the Hikurangi Margin, New Zealand: Review of studies in 2006 and 2007. *Mar. Geol.* doi:10.1016/j.margeo.2010.01.017.
- Han, X., Suess, E., Huang, Y., Wud, N., Bohrmann, G., Su, X., Eisenhauer, A., Rehder, G., Fanga, Y., 2008. Jiulong methane reef: microbial mediation of seep carbonates in the South China Sea. *Mar. Geol.* 249 (3/4), 243–256.
- Henderson, G.M., Anderson, R.F., 2003. Reviews in Mineralogy and Geochemistry 52, 493–531.
- Hovland, M., Thomsen, E., 1997. Cold-water corals – are they hydrocarbon seep related? *Mar. Geol.* 137, 159–164.
- Jones, A.T., Greinert, J., Bowden, D., Klauke, I., Petersen, J., Netzeband, G., Weinrebe, W., this issue. Acoustic and visual characterisation of methane-rich seabed seeps at Omakere Ridge on the Hikurangi Margin, New Zealand. *Mar. Geol.* doi:10.1016/j.margeo.2009.03.008.
- Judd, A.G., 2003. The global importance and context of methane escape from the seabed. *Geo-Mar. Lett.* 23, 147–154.
- Judd, A., Hovland, M., 2007. Seabed Fluid Flow: The impact on Geology, Biology and the Marine Environment. Cambridge University Press, New York. 475 pp.
- Judd, A.G., Hovland, M., Dimitrov, L.L., Gil, S.G., Jukes, V., 2002. The geological methane budget at continental margins and its influence on climate change. *Geofluids* 2, 109–126.
- Klauke, I., Weinrebe, W., Petersen, C.J., Bowden, D., this issue. Temporal variability of gas seeps offshore New Zealand: Multi-frequency geoaoustic imaging of the Wairarapa area, Hikurangi Margin. *Mar. Geol.* doi:10.1016/j.margeo.2009.02.009.
- Kulm, L.D., Suess, E., 1990. Relationship between carbonate deposits and fluid venting: Oregon accretionary prism. *J. Geophys. Res.* 95, 8899–8915.
- Kutterolf, S., Liebetrau, V., Mörz, T., Freundt, A., Hammerich, T., Garbe-Schönberg, D., 2008. Lifetime and cyclicity of fluid venting at forearc mound structures determined by tephrostratigraphy and radiometric dating of authigenic carbonates. *Geology* 36, 707–710, doi:10.1130/G24806A.1.
- LaBonte, A.L., Brown, K.M., Tryon, M.D., 2007. Monitoring periodic and episodic flow events at Monterey Bay seeps using a new optical flow meter. *J. Geophys. Res.* 112, B02105, doi:10.1029/2006JB004410.
- Law, C.S., Nodder, S.D., Mountjoy, J., Marriner, A., Orin, A., Pilditch, C.A., Franz, P., Thomson, K., this issue. Geological, hydrodynamic and biogeochemical variability of a New Zealand deep-water methane cold seep during an integrated Three-year time-series study. *Mar. Geol.* doi:10.1016/j.margeo.2009.06.018.
- Ledersat, B., Buret, C., Chanier, F., Ferriere, J., Recourt, P., 2003. Tubular structures of northern Wairarapa (New Zealand) as possible examples of ancient fluid expulsion in an accretionary prism: evidence from field and petrographical observations. *Geol. Soc. Special Publ.* 386 (216), 95–107.
- Leefmann, T., Bauermeister, J., Kronz, A., Liebetrau, V., Reitner, J., Thiel, V., 2008. Miniaturized biosignature analysis reveals implications for the formation of cold seep carbonates at Hydrate Ridge (off Oregon, USA). *Biogeosciences* 5, 731–738.
- Lewis, K.B., Marshall, B.A., 1996. Seep faunas and other indicators of methane-rich dewatering on New Zealand convergent margins. *N. Z. J. Geol. Geophys.* 39, 181–200.
- Liebetrau, V., Eisenhauer, A., Fietzke, J., Kutterolf, S., Hammerich, T., Günther, D., Linke, P., 2008. Cold-seep carbonates as marine isotope geochemical archives: new insights comparing chronology and emplacement controlling processes of circum-Pacific settings. *Geochim. Cosmochim. Acta* 72, A551.
- Linke, P., Sommer, S., Rovelli, L., McGinnis, D.F., this issue. Physical limitations of dissolved methane fluxes: The role of bottom layer process. *Mar. Geol.* doi:10.1016/j.margeo.2009.03.020.
- Luff, R., Wallman, K., 2003. Fluid flow, methane fluxes, carbonate precipitation and biogeochemical turnover in gas hydrate-bearing sediments at Hydrate Ridge, Cascadia margin: numerical modelling and mass balances. *Geochim. Cosmochim. Acta* 67, 3403–3412.
- Luff, R., Wallmann, K., Aloisi, G., 2004. Numerical modelling of carbonate crust formation at cold vent sites: significance for fluid and methane budgets and chemosynthetic biological communities. *Earth Planet. Sci. Lett.* 221, 337–353.
- Mau, S., Rehder, G., Arroyo, I.G., Gossler, J., Suess, E., 2007. Indications of a link between seismotectonics and CH₄ release from seeps off Costa Rica. *Geochim. Geophys. Geosyst.* 8, Q04003, doi:10.1029/2006GC001326.
- Mienis, F., Stigter, H.C., White, M., Duineveld, G., Haas, H., Weering, T.C.E., 2007. Hydrodynamic controls on cold-water coral growth and carbonate-mound development at the SW and SE Rockall Trough Margin. *NE Atlantic Ocean. Deep-Sea Res.* 54, 1655–1674.
- Netzeband, G.L., Krabbenhöft, A., Zillmer, M., Petersen, C.J., Papenberg, C., Bialas, J., this issue. Seeps and the structures underneath – seismic evidence from the Wairarapa area. *Mar. Geol.* doi:10.1016/j.margeo.2009.07.005.
- Nymann, S.L., Nelson, C.S., Campbell, K.A., this issue. Possible late Miocene analogue for the subsurface plumbing of modern Hikurangi Margin cold seeps: Evidence from tubular concretions in southern Hawke's Bay. *Mar. Geol.* doi:10.1016/j.margeo.2009.03.021.
- Peltier, A., Hurst, T., Scott, B., Cayol, V., 2009. Structures involved in the vertical deformation at Lake Taupo (New Zealand) between 1979 and 2007: new insights from numerical modelling. *Journal of Volcanology and Geothermal Research* 181, 173–184, doi:10.1016/j.jvolgeores.2009.01.017.
- Ponse-Branchu, E., Hillaire-Marcel, C., Deschamps, P., Ghaleb, B., Sinclair, D.J., 2005. Early diagenesis impact on precise U-series dating of deep-sea corals: example of a 100–200-year old *Lophelia pertusa* sample from the northeast Atlantic. *Geochim. Cosmochim. Acta* 69, 4865–4879, doi:10.1016/j.gca.2005.06.011.
- Roberts, J.M., Wheeler, A.J., Freiwald, A., 2006. Reefs of the deep: the biology and geology of cold-water coral ecosystems. *Science* 312, 543–547.
- Roberts, J.M., Wheeler, A.J., Freiwald, A., Cairns, S.D., 2009. Cold-water corals. *The Biology and Geology of Deep-sea Coral Habitats*. Cambridge University Press, Cambridge, p. 336 pp.
- Sauter, E.J., Muyakshin, S.I., Charlou, J.L., Schlüter, M., Boetius, A., Jerosch, K., Damm, E., Foucher, J.P., Klages, M., 2006. Methane discharge from a deep-sea submarine mud volcano into the upper water column by gas hydrate-coated methane bubbles. *Earth Planet. Sci. Lett.* 243, doi:10.1016/j.epsl.2006.01.041.
- Sommer, S., Pfannkuche, O., Linke, P., Luff, R., Greinert, J., Drews, M., Gubsch, S., Pieper, M., Poser, M., Viergutz, T., 2006. Efficiency of the benthic filter: biological control of the emission of dissolved methane from sediment containing shallow gas hydrates at Hydrate Ridge. *Glob. Biogeochem. Cycl.* 20, doi:10.1029/2004GB002389.
- Teichert, B.M.A., Eisenhauer, A., Bohrmann, G., Haase-Schramm, A., Bock, B., Linke, P., 2003. U/Th Systematics and ages of authigenic carbonates from Hydrate Ridge, Cascadia Margin: recorders of fluid flow variations. *Geochim. Cosmochim. Acta* 67 (20), 3845–3857.
- Teichert, B.M.A., Gussone, N., Eisenhauer, A., Bohrmann, G., 2005. Clathrites: archives of near-seafloor pore-fluid evolution ($\delta^{44/40}\text{Ca}$, $\delta^{13}\text{C}$, $\delta^{18}\text{O}$) in gas hydrate environments. *Geology* 33, 213–216.
- Thurber, A.R., Kröger, K., Neira, C., Wiklund, H., Levin, L.A., this issue. Stable isotope signatures and methane use by New Zealand cold seep benthos. *Mar. Geol.* doi:10.1016/j.margeo.2009.06.001.

- Tryon, M.D., Brown, K.M., Torres, M.E., 2002. Fluid and chemical flux in and out of sediments hosting methane hydrate deposits on Hydrate Ridge, OR, II: hydrological processes. *Earth Planet. Sci. Lett.* 201, 541–557.
- Watanabe, Y., Nakai, S., Hiruta, A., Matsumoto, R., Yoshida, K., 2008. U–Th dating of carbonate nodules from methane seeps off Joetsu, Eastern Margin of Japan Sea. *Earth Planet. Sci. Lett.* 272, 89–96.
- Wedepohl, K.H., 1995. The composition of the continental crust. *Geochim. Cosmochim. Acta* 59 (7), 1217–1232.
- White, M., Mohn, C., Stigter, H., Mottram, G., 2005. Deep-water coral development as a function of hydrodynamics and surface productivity around the submarine banks of the Rockall Trough, NE Atlantic. In: Freiwald, A., Roberts, J.M. (Eds.), *Cold-Water Corals and Ecosystems*. Springer, Heidelberg, pp. 503–514.
- Wilson, C.J.N., Houghton, B.F., McWilliams, M.O., Lanphere, M.A., Weaver, S.D., Briggs, R.M., 1995. Volcanic and structural evolution of Taupo Volcanic Zone, New Zealand: a review. *J. Volcanol. Geotherm. Res.* 68, 1–28.